Am J Transl Res 2022;14(12):8934-8946
www.ajtr.org /ISSN:1943-8141/AJTR0146380

Original Article

Gab1 regulates invadopodia and autocrine VEGF through SHP2/ERK1/2 in hilar cholangiocarcinoma cells

Tingting Li[1], Ye Tian[2], Weiqiang Ren[3], Peng Chen[3], Mingxiao Luo[3], Haiquan Sang[3]

[1]Department of Clinical Genetics, Shengjing Hospital of China Medical University, Shenyang 110004, Liaoning, P. R. China; Departments of [2]Thoracic Surgery, [3]General Surgery, The Fourth Affiliated Hospital of China Medical University, Shenyang 110032, Liaoning, P. R. China

Received September 7, 2022; Accepted December 3, 2022; Epub December 15, 2022; Published December 30, 2022

Abstract: Objectives: Hilar cholangiocarcinoma is the most common malignant tumors of the biliary tract and it has high invasiveness. Invadopodia and autocrine vascular endothelial growth factor (VEGF) are closely related to tumor invasiveness. We investigated the role of Grb2-associated binder 1 (Gab1) in invadopodia and autocrine VEGF in hilar cholangiocarcinoma cells. Methods: The expression of Gab1 and vascular endothelial growth factor receptor 2 (VEGFR-2) in tumor cells was detected by real-time PCR. MTT, flow cytometry and transwell assays were used to determine the effect of Gab1 on the biological behavior of tumor cells. In situ gelatin zymogram, western blotting, ELISA and immunofluorescence were used to study Gab1- and apatinib-regulated invadopodia, epithelial-mesenchymal transition (EMT), and VEGF autocrine signaling through the SHP2/ERK1/2 pathway. Results: Gab1 controlled invadopodia maturation via the regulation of cortactin and EMT. Additionally, Gab1-regulated autocrine VEGF was observed in tumor cells expressing VEGFR-2, and endogenous and exogenous VEGF regulated VEGF expression through p-VEGFR-2 nuclear aggregation. Furthermore, the Gab1/SHP2/ERK1/2 axis regulated invadopodia and VEGF autocrine function in tumor cells. Finally, apatinib inhibited the malignant behavior of tumor cells and the nuclear aggregation of p-VEGFR-2 by inhibiting the phosphorylation of VEGFR-2 (direct) and the expression of Gab1 (indirect) in tumor cells. Conclusions: This study demonstrates that Gab1 and apatinib affect tumor cell invadopodia and autocrine VEGF expression through the Gab1/SHP2/ERK1/2 axis in hilar cholangiocarcinoma cells.

Keywords: Hilar cholangiocarcinoma, Gab1, invadopodia, VEGF autocrine, apatinib

Introduction

Hilar cholangiocarcinoma is the most common biliary malignant tumor [1]. Radical surgical resection (R0) is the only existing therapeutic approach [2]. However, the postoperative recurrence rate of hilar cholangiocarcinoma is as high as 76%, and the tumor is not sensitive to adjuvant therapy [1, 3]. Even after R0 resection, the 5-year survival rate of patients is only 19%, while the 5-year survival rate of patients without R0 is almost zero [2, 4].

Grb2-associated binder 1 (Gab1) is the most abundant and widely distributed member of the Gab family [5]. It plays a regulatory role in the transmission and amplification of signals [5]. In our previous study, high expression of Gab1 was found in hilar cholangiocarcinoma [6]. Invadopodia are protruding structures in the cell membrane rich in filamentous actin that are used by tumor cells to invade surrounding tissues and to degrade the extracellular matrix (ECM) [7]. Cortactin phosphorylation, Tks5 and matrix metallopeptidase-9 (MMP-9) participate in processes involved in the maturation of invadopodia [8]. Tumors that express vascular endothelial growth factor receptor 2 (VEGFR-2) exhibit autocrine vascular endothelial growth factor (VEGF) regulation, thereby contributing to tumor formation and angiogenesis [9, 10]. Interestingly, extracellular signal-regulated kinase (ERK) 1/2, which acts downstream of Gab1, regulates cortactin phosphorylation and autocrine VEGF [11, 12].

In this study, we elucidated the relationship between hilar cholangiocarcinoma cell invadopodia and autocrine VEGF with the Gab1/SHP2/ERK1/2 axis and studied the malignant behavior of tumor cells after apatinib treatment.

Materials and methods

Cell lines

Human hilar cholangiocarcinoma cells ICBD-1 (Aiyan Biotech Shanghai Co., Ltd., China) and TFK-1 (BeNa Culture Collection, China) and human intrahepatic bile duct epithelial cells HUM-CELL-0035 (Wuhan Primary Biopharmaceutical Technology Co., Ltd., China) were cultured in DMEM containing 10% fetal bovine serum (FBS). In VEGF autocrine experiments, cells were incubated for 24 h, and the medium was replaced with DMEM containing 2% FBS to continue culture.

Real-time PCR

Cultured cells at 90% density were collected and treated with 1 ml TRIpure lysate and 200 μl chloroform for 3 min. Then, the cells were centrifuged to obtain the water phase. After the addition of isopropanol and 75% ethanol, the samples were centrifuged, and DEPC water was added to obtain the total RNA of the samples. The obtained RNA was reverse transcribed to acquire cDNA. A real-time quantitative PCR system was established, and the results were analysed by the ExicyclerTM 96 (BIONEER, Korea). Primers were synthesized by Sangon Biotech (Shanghai) Co., Ltd. Gab1-F, TTGTGACATCTGTGGGTTTA; Gab1-R, GTGGTGGAACATTGATTAGC; VEGFR-2-F, CAATAATCAGAGTGGCAGTG; VEGFR-2-R, TAGACATAAATGACCGAGGC.

siRNA interference and vector construction

Four Gab1 siRNAs and one negative control (NC) were transfected into the cells (2 μg/ml). After 48 h, cellular RNA was extracted for real-time PCR, and the siRNA with the highest interference efficiency was selected. According to the human Gab1 gene (NM_207123.2), the Gab1 wild-type overexpression vector Gab1-WT (which led to an increase in Gab1 expression in cells), the Gab1 mutant expression vector Gab1-ΔSHP2 (Tyr627 and Tyr659 of Gab1 were mutated, which were the necessary binding sites for SHP2), and its control Empty-vector were transfected into cells. The interference sequences and expression vectors were synthesized by Sangon Biotech (Shanghai) Co., Ltd.

Western blotting

Protein extraction (Wanleibio, China) was performed for quantification (BSA protein standard solution) and transferred to PVDF membranes after SDS-PAGE electrophoresis (40 μg). Then, the membranes were blocked with 5% milk or 1% BSA and incubated with primary antibodies overnight and secondary antibodies for 45 min. The membranes were incubated with luminescent solution for exposure. After antibody stripping, PVDF membranes were incubated again with the internal reference antibody and secondary antibody and were incubated with luminescent solution for exposure. The Gel-Pro-Analyser system was used to analyse the results. Antibodies against Gab1 (Santa Cruz, USA), VEGFR-2 (Abclonal, China), MMP-9, cortactin and Tks5 (Proteintech, China), ERK1/2, E-cadherin, N-cadherin and Vimentin (Wanleibio, China) were used.

MTT assay

The cells from each group were inoculated at a concentration of 1×10^4 cells per well. This time was considered to be 0 h. In addition, after 24, 48, and 72 h, the MTT test (KeyGEN, China) was performed. The medium containing 0.5 mg/ml MTT was replaced with medium, and the cells were incubated for 4 h. The supernatant was absorbed, and 150 μl DMSO was added. After standing 10 for min in the absence of light, the optical density at 570 nm was measured on the enzyme-labelled instrument.

Cell cycle detection

Cells in each group were collected after centrifugation, and precooled 70% ethanol was added to fix the cells at 4°C for 2 h. The cells were centrifuged again, 100 μl RNase A was added, and the mixture was incubated at 37°C for 30 min. After adding 500 μl of propidium iodide staining solution, the mixture was incubated in the dark at 4°C for 30 min. Then, flow cytometry was performed (NovoCyte, Aceabio, USA).

Transwell assay

A total of 800 μl of culture medium containing 20% FBS was added to the lower chamber of the Transwell (Corning, USA), and 200 μl of cells with a cell density adjusted to 2.5×10^5 cells/mL was added to the upper chamber. The cells were cultured for 24 h, fixed with 4% paraformaldehyde for 25 min, and stained. The cells that migrated to the lower layer of the microporous membrane were counted under an inverted microscope (200 ×). Five fields were selected for each sample to count the number of cells, and the average was taken.

In situ gelatin zymography to detect invadopodia

Gelatin labelled with FITC was established [13]. The cells of each group were cultured in a 24-well plate containing treated cover slips with cells at a density of 2.5×10^4 cells/well. The cells were fixed, and rhodamine phalloidin was used to label the cytoskeleton (Cytoskeleton, USA) and incubated for 20 min. After the stain was cleared, diluted DAPI (5 μg/ml) was added to the cells to stain the nucleus. After eliminating DAPI, the anti-fluorescence quencher was added to the cover slips and reversed on a glass slide. The staining was observed under a fluorescence laser confocal microscope (OLUMPUS, Japan) and photographed under a magnification of 600X.

Detection of VEGF and MMP-9 in the supernatant

The diluted VEGF and MMP-9 standards were added to the 96-well plate along with 100 μl of the diluted sample for detection (Wanleibio, China). The capture antibody was added at a volume of 100 μl. Diluted HRP-streptavidin (100 μl) was added after washing the plate, and 100 μl TMB chromogenic solution was added to each well and incubated for 15 min after washing the plate again. TMB stop solution (50 μl) was added to stop the reaction, and the absorbance was read at 450 nm with a microplate reader. Taking the standard concentration (pg/ml) as the ordinate and the OD as the abscissa, a linear regression curve of the standard was drawn. The concentration of each sample was calculated according to the curve equation.

Immunofluorescence for the detection of protein localization

The cells of each group were fixed and incubated with the primary antibody overnight at 4°C. The primary antibody was washed, and the fluorescent secondary antibody was dropped on the cells at a dilution ratio of 1:400 protected from light and incubated at room temperature for 45 min. The secondary antibody was removed, and DAPI was added to the cells to stain the nuclei. The DAPI was then washed, and an anti-fluorescence quencher was placed on the cover glass. The staining was observed under a fluorescence laser confocal microscope (OLUMPUS, Japan) and photographed under a magnification of 600X. Antibodies against Gab1 (Santa Cruz, USA), VEGFR-2 (Abclonal, China) and cortactin (Proteintech, China) were used.

Statistical analysis

IBM SPSS 19 (SPSS, Inc., USA) was used for statistical analysis. All data (obtained from three independent experiments) are expressed as the mean ± standard deviation ($\bar{x} \pm s$), and the independent sample t-test was used to compare the mean between the two groups. $P < 0.05$ indicated statistical significance.

Results

Gab1 regulates the maturation of invadopodia in hilar cholangiocarcinoma cells

Our previous study confirmed that VEGFR-2, Gab1, and MMP-9 were overexpressed in hilar cholangiocarcinoma tissues [6]. Thereafter, we found that compared with HUM-CELL-0035 cells, the expression of Gab1 and VEGFR-2 mRNA in ICBD-1 and TFK-1 cells was higher (**Figure 1A**). Gab1 regulated the proliferation, cell cycle progression and invasion of ICBD-1 and TFK-1 cells (**Figures 1B-E**, **4D-F**) [6].

The invasion ability of tumor cells is closely related to the exhibition of invadopodia [7]. Compared with Empty-vector cells, increased cytoskeletal accumulation was observed at the edge of the cells in the Gab1-WT groups of ICBD-1 and TFK-1 cells (**Figure 2A**). Additionally, gelatin degradation around the cytoskeleton in Gab1-WT cells tended to increase (**Figure 2A**).

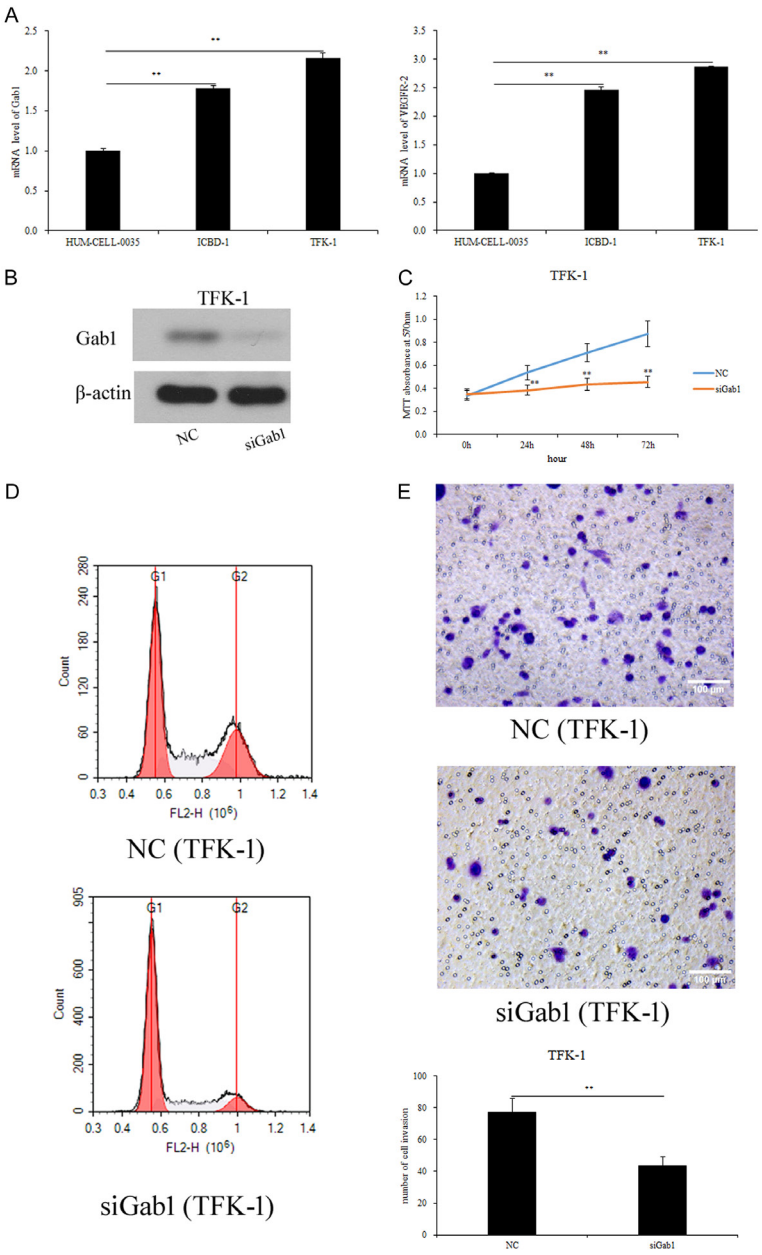

Figure 1. Downregulation of Gab1 affects the malignant behavior of hilar cholangiocarcinoma cells. A. Real-time PCR detected the expression of Grb2-associated binder 1 (Gab1) and vascular endothelial growth factor receptor 2 (VEGFR-2) in HUM-CELL-0035, ICBD-1 and TFK-1 cells. B-E. Compared with the negative control (NC) group, TFK-1 cells in the siGab1 group showed decreased proliferation, arrested cell cycle in the G1 phase, and decreased cell invasion. $^{**}P < 0.01$.

As the major components in invadopodia maturation, p-cortactin and Tks5 were observed [8]. Cortactin phosphorylation decreased in the siGab1 group and increased in the Gab1-WT group of both tumor cells, but the change in Gab1 expression did not affect the expression of cortactin in all tumor cells (**Figure 2B**). Similarly, the expression of Tks5 decreased in the siGab1 group and increased in the Gab1-WT group of both tumor cell lines (**Figure 2C**).

MMP-9 is a critical protein for invadopodia maturation and invadopodia-mediated ECM degradation [8]. Compared with the Empty-vector group, the expression of MMP-9 in the Gab1-WT group of both tumor cells increased, but the expression of pro-MMP-9, the inactive precursor of MMP-9, did not change (**Figure 2D**, **2E**). Meanwhile, compared with the NC group, the expression of MMP-9 in TFK-1 cells decreased upon Gab1 knockdown, whereas the expression of pro-MMP-9 did not change (**Figure 2E**), which was consistent with that observed in ICBD-1 cells [6]. Additionally, ELISA analysis showed that the content of MMP-9 in the supernatant of both tumor cell lines decreased in the siGab1 group and increased in the Gab1-WT group (**Figure 2F**). Furthermore, the merged signal between Gab1 and p-cortactin (an invadopodia marker) was detected near the cell membrane. Compared with the Empty-vector group, the merged signal increased in the Gab1-WT group of both tumor cells (**Figure 2G**). Epithelial-mesenchymal transition (EMT) promotes the maturation of invadopodia [14]. The expression of the epithelial marker E-cadherin increased, whereas the expression of mesenchymal markers such as N-cadherin and vimentin decreased upon Gab1 knockdown in both tumor cell lines (**Figure 2H**). In contrast, the expression of E-cadherin decreased while the expression of N-cadherin

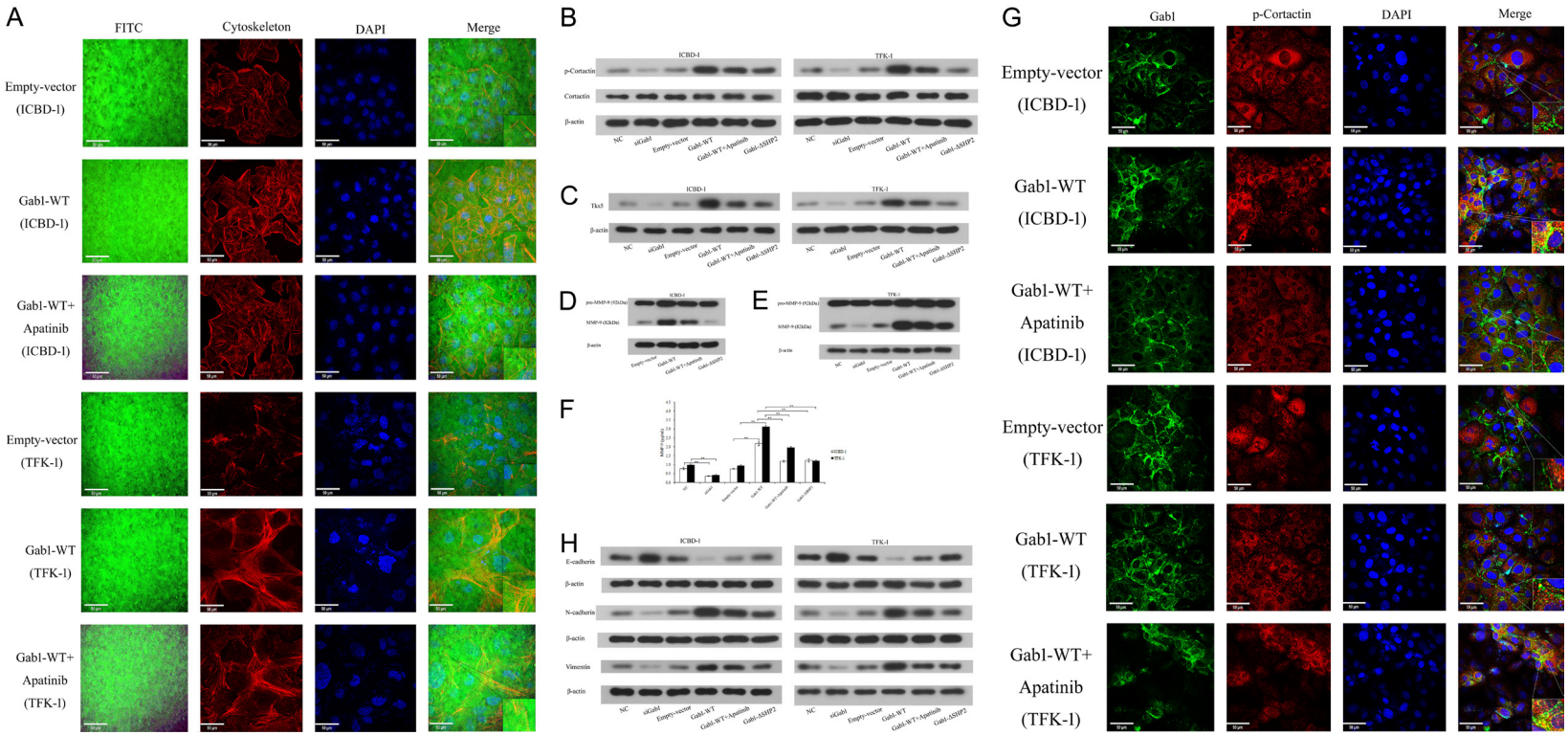

Figure 2. Gab1 regulates the maturation of invadopodia in hilar cholangiocarcinoma cells through SHP2, and apatinib inhibits Gab1-mediated invadopodia maturation in tumor cells. A. Cytoskeletal (red) and extracellular matrix (green) degradation in ICBD-1 and TFK-1 cells was detected by in situ gelatin zymography. B. Western blot detection of the effect of Gab1 and apatinib on the phosphorylation level of cortactin in tumor cells. C. The effects of Gab1 and apatinib on the protein level of Tks5 in tumor cells were detected by western blot. D-F. The changes in matrix metallopeptidase-9 (MMP-9) at the protein level and supernatant content in each group were detected by western blotting and ELISA. G. The intracellular distribution changes of Gab1 (green) and p-cortactin (red) in tumor cells were detected by immunofluorescence. H. The effects of Gab1 and apatinib on epithelial-mesenchymal transition (EMT) markers were detected by western blot. $^{**}P < 0.01$.

and vimentin increased in the Gab1-WT group of both tumor cell lines (**Figure 2H**).

Gab1 regulates VEGF autocrine signaling in hilar cholangiocarcinoma cells

Tumors expressing VEGFR-2 exhibit autocrine VEGF [9]. We found that VEGFR-2 was overexpressed in hilar cholangiocarcinoma tissues and cells (**Figure 1A**) and that VEGFR-2 affected the malignant tumor behavior of hilar cholangiocarcinoma through Gab1 expression [6]. As described in the Methods section, the cells in the VEGF autocrine experiments were cultured in DMEM containing 2% FBS. VEGFR-2 phosphorylation in ICBD-1 and TFK-1 cells in the siGab1 group was lower than that in the NC group, while VEGFR-2 phosphorylation in both tumor cells in the Gab1-WT group was higher than that in the Empty-vector group (**Figure 3A**, **3B**). The expression of Gab1 did not affect the expression of VEGFR-2 in either tumor cell (**Figure 3A**, **3B**). Additionally, compared with the NC group, the levels of VEGF-A and VEGF-C, the main ligands of VEGFR-2, in the supernatant of both tumor cells in the siGab1 group decreased, while they increased in the Gab1-WT group compared to that of the Empty-vector group (**Figure 3C**, **3D**). Autocrine VEGF continuously activates VEGFR-2 phosphorylation and nuclear aggregation of p-VEGFR-2, which increases the expression of VEGF [9]. We found that the change in Gab1 expression changed the distribution of p-VEGFR-2 in cells. Compared with the Empty-vector group, p-VEGFR-2 translocated to the cytoplasm and nucleus, and nuclear aggregation of p-VEGFR-2 increased in the Gab1-WT group of both tumor cell lines (**Figure 3E**). Furthermore, we administered exogenous VEGF-A to simulate VEGF in the microenvironment of cholangiocarcinoma [15]. Five minutes after the addition of VEGF-A (50 ng/mL) to each group, the Gab1-WT group in both tumor cells showed more p-VEGFR-2 migration and nuclear aggregation than the Empty-vector group (**Figure 3F**).

The Gab1/SHP2/ERK1/2 axis regulates VEGF autocrine and malignant behavior in hilar cholangiocarcinoma cells

ERK1/2 plays a key role in the phosphorylation of cortactin in invadopodia, EMT, and autocrine VEGF regulation [11, 12, 16]. Previously, we confirmed that VEGFR-2 in ICBD-1 affected PI3K/Akt activity through Gab1 expression [6]. Additionally, it was shown that Gab1/SHP2 regulated ERK1/2 and that there was positive feedback between the Gab1/ERK1/2 and Gab1/PI3K/Akt signaling pathways in cells [5, 17, 18]. We found that the phosphorylation of ERK1/2 decreased in the siGab1 group and increased in the Gab1-WT group of ICBD-1 and TFK-1 cells. However, changes in Gab1 did not affect the expression of ERK1/2 in either tumor cell (**Figure 4A**, **4B**). Meanwhile, compared with the Gab1-WT group, the phosphorylation levels of ERK1/2 in the Gab1-ΔSHP2 of both tumor cells decreased, whereas they showed no effect on ERK1/2 expression (**Figure 4A**, **4B**). Furthermore, compared with the Gab1-WT group, VEGFR-2 phosphorylation decreased in the Gab1-ΔSHP2 group of both tumor cells, but the VEGFR-2 expression level was not affected (**Figure 3A**, **3B**). Similarly, compared with the Gab1-WT group, apatinib, a highly selective VEGFR-2 inhibitor, also reduced the phosphorylation levels of VEGFR-2 and ERK1/2 in the Gab1-WT group of both tumor cells in low-concentration medium (**Figures 3A**, **3B**, **4A**, **4B**). Apatinib showed no change in the expression of ERK1/2 and VEGFR-2 (**Figures 3A**, **3B**, **4A**, **4B**). Interestingly, compared with the Gab1-WT group, apatinib treatment decreased the expression of Gab1 in both tumor cell lines (**Figure 4C**). Additionally, compared with the Gab1-WT group, cell proliferation decreased, the cell cycle was arrested in the G1 phase, and cell invasion decreased in the Gab1-ΔSHP2 group of both tumor cells (**Figure 4D-F**). The cell proliferation assay showed that apatinib functioned after 48 h (**Figure 4D**). The apatinib-treated Gab1-WT group exhibited a phenotype similar to that of the Gab1-ΔSHP2 group (**Figure 4D-F**).

Apatinib inhibits invadopodia and autocrine VEGF in hilar cholangiocarcinoma cells through the regulation of the Gab1/SHP2/ERK1/2 axis

We further investigated the effects of the Gab1/SHP2/ERK1/2 axis and apatinib on invadopodia and VEGF autocrine signaling in tumor cells. Compared with the Gab1-WT group, apatinib reduced cytoskeletal accumulation at the edge of the cells in the Gab1-WT group of ICBD-1 and TKF-1 cells, and the degradation of gelatin around the cytoskeleton tended to decrease (**Figure 2A**). Moreover, compared with the

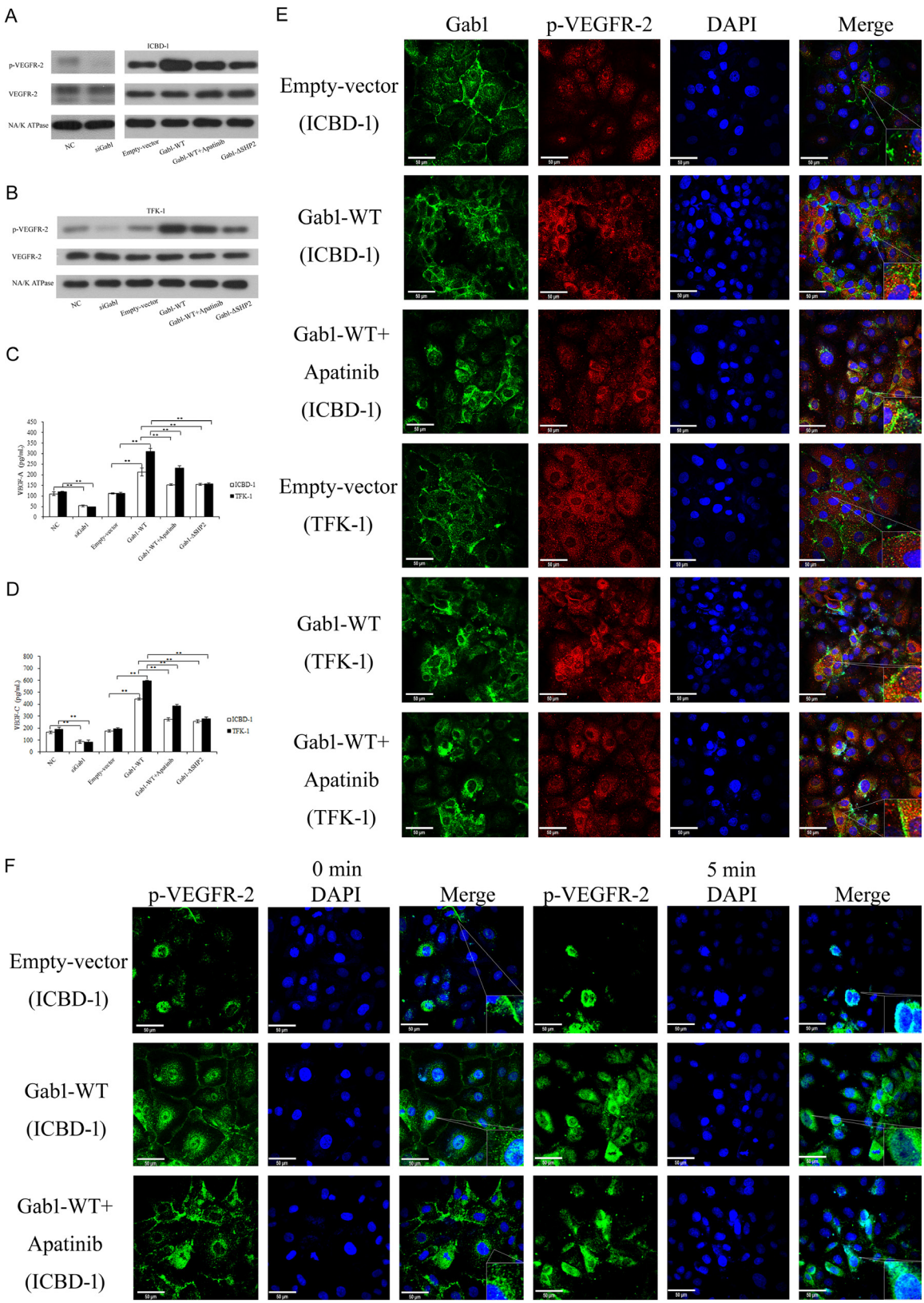
A
ICBD-1
p-VEGFR-2
VEGFR-2
NA/K ATPase
NC
siGab1
Empty-vector
Gab1-WT
Gab1-WT+Apatinib
Gab1-ΔSHP2
B
TFK-1
C
VEGF-A (pg/mL)
ICBD-1
TFK-1
D
VEGF-C (pg/mL)
E
Gab1
p-VEGFR-2
DAPI
Merge
Empty-vector (ICBD-1)
Gab1-WT (ICBD-1)
Gab1-WT+ Apatinib (ICBD-1)
Empty-vector (TFK-1)
Gab1-WT (TFK-1)
Gab1-WT+ Apatinib (TFK-1)
F
0 min
5 min
p-VEGFR-2
DAPI
Merge
Empty-vector (ICBD-1)
Gab1-WT (ICBD-1)
Gab1-WT+ Apatinib (ICBD-1)

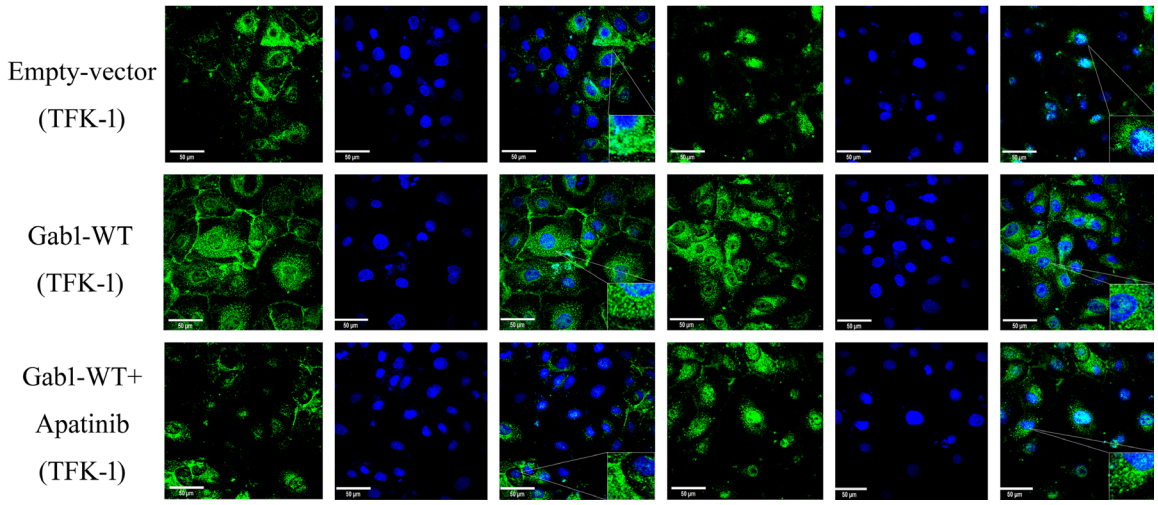

Figure 3. Gab1 regulates autocrine vascular endothelial growth factor (VEGF) in hilar cholangiocarcinoma cells through nuclear aggregation of p-VEGFR-2, and apatinib inhibits Gab1-mediated autocrine VEGF in tumor cells via SHP2. The cells were cultured in DMEM containing 2% fetal bovine serum (FBS). A, B. Western blot detection of the effect of Gab1 and apatinib on the phosphorylation level of VEGFR-2 in ICBD-1 and TFK-1 cells. C, D. The content of VEGF-A and VEGF-C in the supernatant of each group was detected by ELISA. E. The intracellular distribution of Gab1 and p-VEGFR-2 in tumor cells was detected by immunofluorescence. F. Immunofluorescence detected the effect of exogenous VEGF and apatinib on the intracellular distribution of p-VEGFR-2 in tumor cells. $^{**}P < 0.01$.

Gab1-WT group, cortactin phosphorylation and Tks5 expression decreased in the Gab1-ΔSHP2 and apatinib-treated Gab1-WT groups of both tumor cell lines (**Figure 2B**, **2C**). However, Gab1/SHP2 and apatinib exerted no effect on the expression of cortactin in either tumor cell (**Figure 2B**). Additionally, compared with the Gab1-WT group, the expression of MMP-9 in the Gab1-ΔSHP2 and apatinib-treated Gab1-WT groups decreased in both tumor cell lines, whereas the expression of pro-MMP-9 did not change (**Figure 2D**, **2E**). Similarly, compared with the Gab1-WT group, the level of MMP-9 in the supernatant of the Gab1-ΔSHP2 and apatinib-treated Gab1-WT groups in both tumor cell lines decreased (**Figure 2F**). Meanwhile, the distribution and overlap of Gab1 and p-cortactin near the cell membrane decreased in the apatinib-treated Gab1-WT group of both tumor cells compared to those in the Gab1-WT group (**Figure 2G**). In contrast, the expression of E-cadherin in the Gab1-ΔSHP2- and apatinib-treated Gab1-WT groups of both tumor cells increased compared to that in the Gab1-WT group, whereas the expression of N-cadherin and vimentin decreased (**Figure 2H**).

Compared with the Gab1-WT group, the levels of VEGF-A and VEGF-C in the supernatant of the Gab1-ΔSHP2 and apatinib-treated Gab1-WT groups in both tumor cells were decreased (**Figure 3C**, **3D**). Furthermore, compared with the Gab1-WT group, apatinib resulted in p-VEGFR-2 translocation to the cytoplasm and cell membrane, and p-VEGFR-2 nuclear aggregation decreased in the Gab1-WT group of both tumor cells (**Figure 3E**). Compared with the Gab1-WT group, apatinib induced p-VEGFR-2 distribution toward the cell membrane and cytoplasm after the addition of exogenous VEGF-A (50 ng/mL) for 5 min (**Figure 3F**). Additionally, p-VEGFR-2 nuclear aggregation decreased in the Gab1-WT group of both tumor cells (**Figure 3F**).

Discussion

Invadopodia explain the invasion ability of tumor cells [7]. Phosphorylated cortactin, Tks5, and MMP-9 are located in invadopodia and are important for invadopodia maturation [8]. Gab1 is an adaptor protein that lacks enzymatic activity [5]. After activation, it can function as a platform for components involved in signal transduction pathways, thus leading to tumor cell survival, proliferation, and differentiation [5]. Studies have found that downregulation of Gab1 expression in monocytes can inhibit cortactin-related cytoskeleton formation and thus inhibit cell migration, whereas overexpression

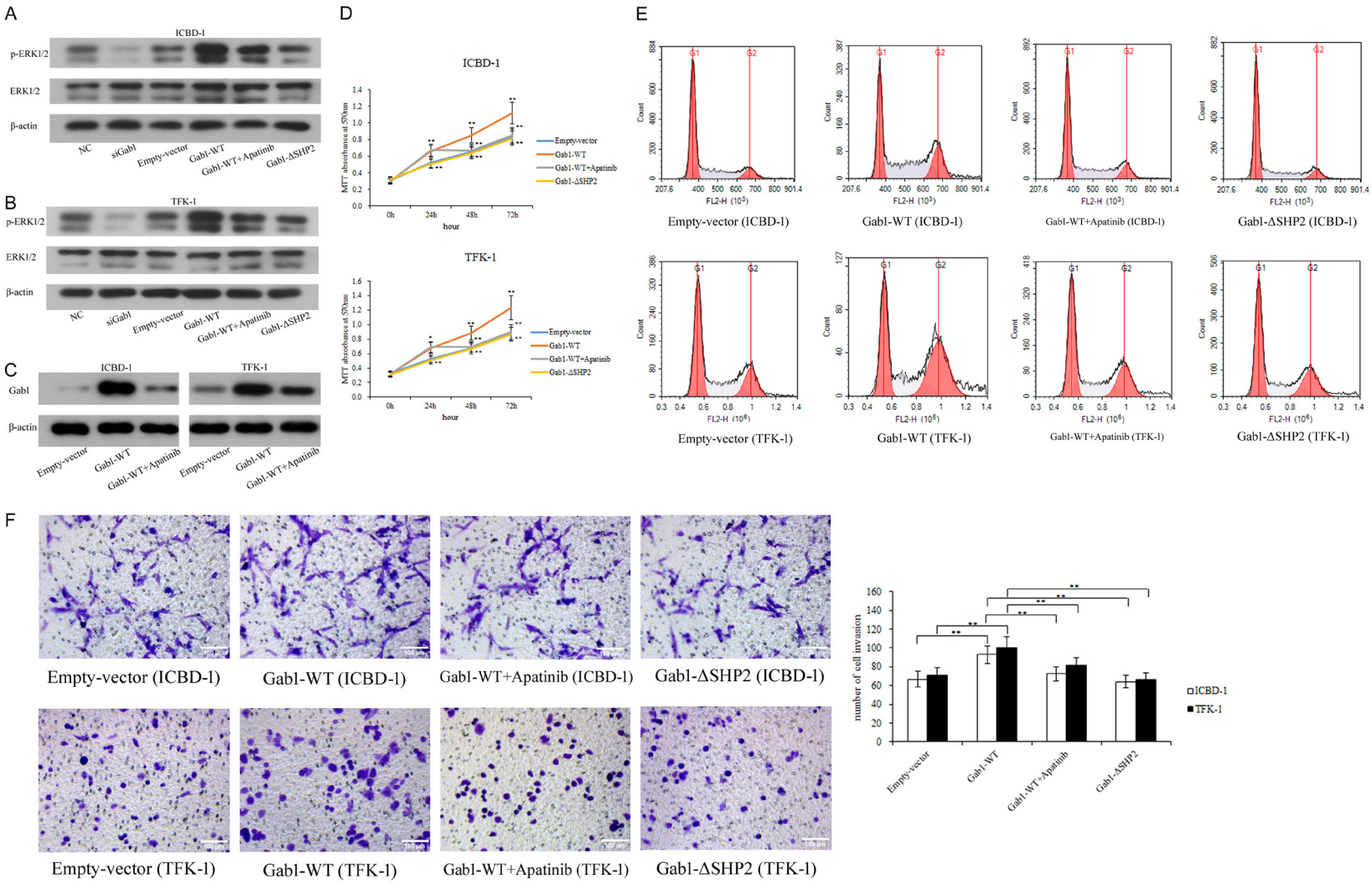

Figure 4. Gab1 regulates the function of hilar cholangiocarcinoma cells through the SHP2/ERK1/2 axis. A, B. Western blot detection of the effect of Gab1/SHP2 and apatinib on the phosphorylation level of extracellular signal-regulated kinase (ERK)1/2 in ICBD-1 and TFK-1 cells. C. Western blot detection of the effect of apatinib on the protein level of Gab1 in tumor cells. D-F. The effects of Gab1/SHP2 and apatinib on proliferation, cell cycle and invasion were detected by MTT, flow cytometry and Transwell assays. *$P < 0.05$, **$P < 0.01$.

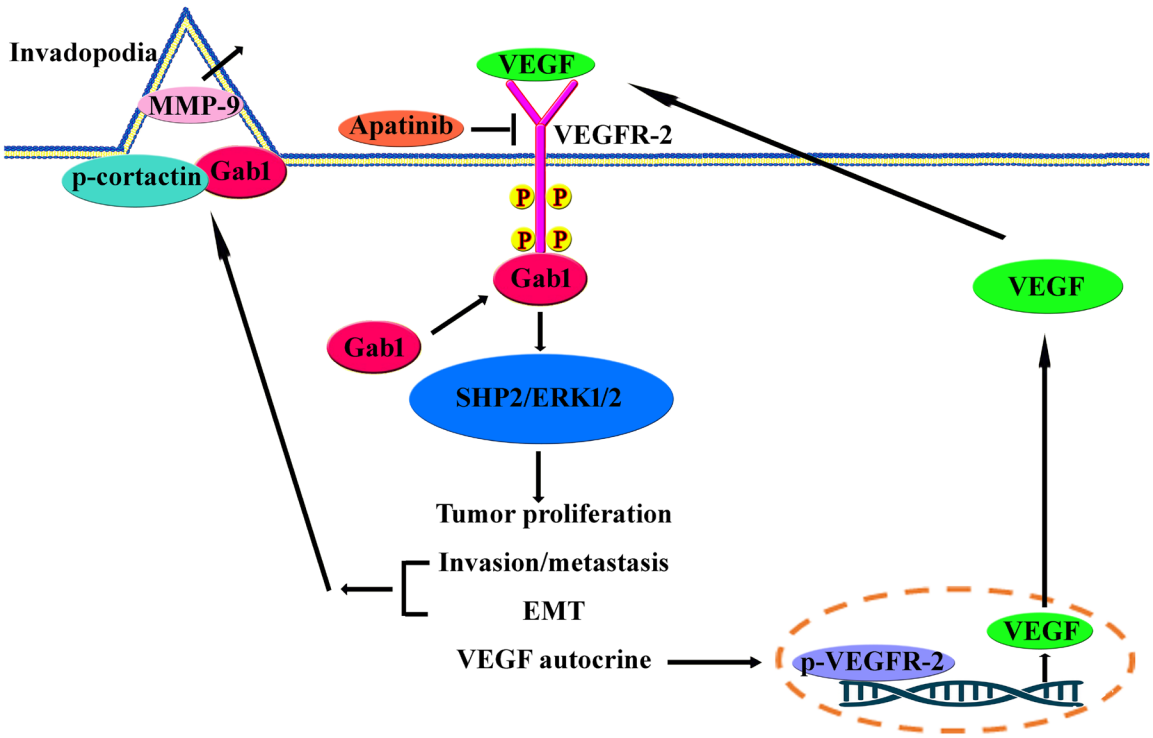

Figure 5. Schematic diagram of Gab1 regulating invadopodia and autocrine VEGF in hilar cholangiocarcinoma cells.

of cortactin and phosphorylation promote pancreatic ductal adenocarcinoma metastasis [19, 20]. Furthermore, the interaction between Gab1 and cortactin near the cell membrane affects the maturation of invadopodia [21]. We found that Gab1 regulated PI3K/Akt activity in hilar cholangiocarcinoma cells, and a positive feedback mechanism between the Gab1/ERK1/2 and Gab1/PI3K/Akt signaling pathways in HEK cells transfected with Gab1 was reported [6, 18]. Gab1/SHP2 regulates the activity of ERK1/2 and participates in the regulation of cortactin phosphorylation and Tks5 and MMP-9 expression [5, 11, 17, 22, 23]. Similarly, we found that Gab1 regulated the phosphorylation of cortactin, the expression of Tks5 and MMP-9 (82 kDa), and the levels of MMP-9 in the supernatant of tumor cells through SHP2/ERK1/2 signaling, thereby regulating invadopodia maturation in tumor cells through the interaction between Gab1 and p-cortactin near the cell membrane. Interestingly, the Gab1/SHP2/ERK1/2 axis did not change the expression of pro-MMP9 (92 kDa). Inactive pro-MMP-9 requires multiple agonists for transformation into active MMP-9 [24]. Sinha et al. reported that cortactin regulates intracellular transport and vesicle release of MMP-9-containing vesicles, while Beghein et al. reported that extracellular vesicles are not necessary for the release of MMP-9 from invadopodia [25, 26]. The mechanism of recruitment, activation, and release of MMP-9 by invadopodia of hilar cholangiocarcinoma cells warrants further study. EMT promotes the maturation of invadopodia in tumor cells [14]. Studies have found that Gab1 is an important factor in the initiation of EMT in hepatocellular carcinoma cells [27]. We also found that the Gab1/SHP2/ERK1/2 axis is involved in the EMT of hilar cholangiocarcinoma cells and promotes the maturation of invadopodia.

A substantial amount of VEGF in the tumor microenvironment is derived from the secretion of tumor cells, and tumors that express VEGFR-2 demonstrate autocrine VEGF regulation [9, 28]. Autocrine VEGF activates VEGFR-2 on the surface of tumor cells to promote self-proliferation and invasion, and VEGFR-2 acts on the surface of endothelial cells, thereby triggering neovascularization [10, 28]. We found VEGFR-2 overexpression in human hilar cholangiocarcinoma and in ICBD-1 and TFK-1 cells [6]. Gab1 and VEGFR-2 form a complex in endothelial cells and activate ERK1/2 to promote angio-

genesis [29]. We found that Gab1 regulated autocrine VEGF through SHP2/ERK1/2 in both tumor cell lines. In endothelial and hepatocellular carcinoma cells, autocrine VEGF binds to VEGFR-2 to induce its phosphorylation and transfer from the cell membrane to the nucleus, and p-VEGFR-2 binds to the promoter in the nucleus to regulate its own transcription [9, 30]. VEGF in the tumor microenvironment of cholangiocarcinoma can also be derived from other cells in the microenvironment, such as cancer-associated fibroblasts (CAFs), which also play an important role in regulating tumor behavior [15]. We also found that Gab1 regulated the translocation and nuclear accumulation of p-VEGFR-2 in both tumor cells and finally affected the changes in VEGF-A and VEGF-C contents in the supernatant, whereas exogenous VEGF showed a synergistic effect.

Apatinib selectively blocks VEGFR-2 phosphorylation in tumor and endothelial cells and inhibits tumor-related angiogenesis [31]. Consistently, we found that apatinib directly inhibited VEGFR-2 phosphorylation in tumor cells, eventually reducing their malignant behavior through the Gab1/SHP2/ERK1/2 axis and p-VEGFR-2 nuclear aggregation induced by auto and exogenous VEGF. Interestingly, apatinib reduced the expression of Gab1, which indirectly affected the malignant biological behavior of tumor cells. The mechanism of the effect of apatinib on Gab1 expression will be the focus of our future research.

Conclusions

In summary, we confirmed that Gab1 regulates tumor cell invadopodia, EMT, and autocrine VEGF through Gab1/SHP2/ERK1/2 in hilar cholangiocarcinoma cells and that apatinib inhibits the above biological behaviors (**Figure 5**).

Acknowledgements

The study was funded by the Youth Fund Project of National Natural Science Foundation of China (Grant No. 81001091), Natural Science Project of Liaoning Provincial Department of Science and Technology (Grant No. 201501018 and 2020-MS-12), Natural Science Project of Liaoning Provincial Department of Education (Grant No. JCZR2020016) and Natural Science Foundation of Tibet Autonomous Region (Grant No. XZ2020ZR-ZY81(Z)).

Disclosure of conflict of interest

None.

Address correspondence to: Tingting Li, Department of Clinical Genetics, Shengjing Hospital of China Medical University, No. 36, Sanhao Street, Heping District, Shenyang 110004, Liaoning, P. R. China. Tel: +86-18940258007; E-mail: litingting0207@126.com; Haiquan Sang, Department of General Surgery, The Fourth Affiliated Hospital of China Medical University, No. 4, Chongshan East Road, Huanggu District, Shenyang 110032, Liaoning, P. R. China. Tel: +86-18900915343; E-mail: sanghaiquan0725@hotmail.com

References

[1] Banales JM, Marin JJG, Lamarca A, Rodrigues PM, Khan SA, Roberts LR, Cardinale V, Carpino G, Andersen JB, Braconi C, Calvisi DF, Perugorria MJ, Fabris L, Boulter L, Macias RIR, Gaudio E, Alvaro D, Gradilone SA, Strazzabosco M, Marzioni M, Coulouarn C, Fouassier L, Raggi C, Invernizzi P, Mertens JC, Moncsek A, Rizvi S, Heimbach J, Koerkamp BG, Bruix J, Forner A, Bridgewater J, Valle JW and Gores GJ. Cholangiocarcinoma 2020: the next horizon in mechanisms and management. Nat Rev Gastroenterol Hepatol 2020; 17: 557-588.

[2] Tran TB, Ethun CG, Pawlik TM, Schmidt C, Beal EW, Fields RC, Krasnick B, Weber SM, Salem A, Martin RCG, Scoggins CR, Shen P, Mogal HD, Idrees K, Isom CA, Hatzaras I, Shenoy R, Maithel SK and Poultsides GA. Actual 5-year survivors after surgical resection of Hilar cholangiocarcinoma. Ann Surg Oncol 2019; 26: 611-618.

[3] Groot Koerkamp B, Wiggers JK, Allen PJ, Besselink MG, Blumgart LH, Busch OR, Coelen RJ, D'Angelica MI, DeMatteo RP, Gouma DJ, Kingham TP, Jarnagin WR and van Gulik TM. Recurrence rate and pattern of perihilar cholangiocarcinoma after curative intent resection. J Am Coll Surg 2015; 221: 1041-1049.

[4] Valle JW, Lamarca A, Goyal L, Barriuso J and Zhu AX. New horizons for precision medicine in biliary tract cancers. Cancer Discov 2017; 7: 943-962.

[5] Wang W, Xu S, Yin M and Jin ZG. Essential roles of Gab1 tyrosine phosphorylation in growth factor-mediated signaling and angiogenesis. Int J Cardiol 2015; 181: 180-184.

[6] Sang H, Li T, Li H and Liu J. Down-regulation of Gab1 inhibits cell proliferation and migration

in hilar cholangiocarcinoma. PLoS One 2013; 8: e81347.
[7] Paterson EK and Courtneidge SA. Invadosomes are coming: new insights into function and disease relevance. FEBS J 2018; 285: 8-27.
[8] Eddy RJ, Weidmann MD, Sharma VP and Condeelis JS. Tumor cell invadopodia: invasive protrusions that orchestrate metastasis. Trends Cell Biol 2017; 27: 595-607.
[9] Peng S, Wang Y, Peng H, Chen D, Shen S, Peng B, Chen M, Lencioni R and Kuang M. Autocrine vascular endothelial growth factor signaling promotes cell proliferation and modulates sorafenib treatment efficacy in hepatocellular carcinoma. Hepatology 2014; 60: 1264-1277.
[10] Szabo E, Schneider H, Seystahl K, Rushing EJ, Herting F, Weidner KM and Weller M. Autocrine VEGFR1 and VEGFR2 signaling promotes survival in human glioblastoma models in vitro and in vivo. Neuro Oncol 2016; 18: 1242-1252.
[11] Schnoor M, Stradal TE and Rottner K. Cortactin: cell functions of a multifaceted actin-binding protein. Trends Cell Biol 2018; 28: 79-98.
[12] Zhang Q, Yu C, Peng S, Xu H, Wright E, Zhang X, Huo X, Cheng E, Pham TH, Asanuma K, Hatanpaa KJ, Rezai D, Wang DH, Sarode V, Melton S, Genta RM, Spechler SJ and Souza RF. Autocrine VEGF signaling promotes proliferation of neoplastic Barrett's epithelial cells through a PLC-dependent pathway. Gastroenterology 2014; 146: 461-472, e6.
[13] Greco MR, Antelmi E, Busco G, Guerra L, Rubino R, Casavola V, Reshkin SJ and Cardone RA. Protease activity at invadopodial focal digestive areas is dependent on NHE1-driven acidic pHe. Oncol Rep 2014; 31: 940-946.
[14] Dongre A and Weinberg RA. New insights into the mechanisms of epithelial-mesenchymal transition and implications for cancer. Nat Rev Mol Cell Biol 2019; 20: 69-84.
[15] Cadamuro M, Brivio S, Mertens J, Vismara M, Moncsek A, Milani C, Fingas C, Cristina Malerba M, Nardo G, Dall'Olmo L, Milani E, Mariotti V, Stecca T, Massani M, Spirli C, Fiorotto R, Indraccolo S, Strazzabosco M and Fabris L. Platelet-derived growth factor-D enables liver myofibroblasts to promote tumor lymphangiogenesis in cholangiocarcinoma. J Hepatol 2019; 70: 700-709.
[16] Fung TM, Ng KY, Tong M, Chen JN, Chai S, Chan KT, Law S, Lee NP, Choi MY, Li B, Cheung AL, Tsao SW, Qin YR, Guan XY, Chan KW and Ma S. Neuropilin-2 promotes tumourigenicity and metastasis in oesophageal squamous cell carcinoma through ERK-MAPK-ETV4-MMP-E-cadherin deregulation. J Pathol 2016; 239: 309-319.
[17] Liu YN, Guan Y, Shen J, Jia YL, Zhou JC, Sun Y, Jiang JX, Shen HJ, Shu Q, Xie QM and Xie Y. Shp2 positively regulates cigarette smoke-induced epithelial mesenchymal transition by mediating MMP-9 production. Respir Res 2020; 21: 161.
[18] Wolf A, Eulenfeld R, Bongartz H, Hessenkemper W, Simister PC, Lievens S, Tavernier J, Feller SM and Schaper F. MAPK-induced Gab1 translocation to the plasma membrane depends on a regulated intramolecular switch. Cell Signal 2015; 27: 340-352.
[19] Gadepalli R, Kotla S, Heckle MR, Verma SK, Singh NK and Rao GN. Novel role for p21-activated kinase 2 in thrombin-induced monocyte migration. J Biol Chem 2013; 288: 30815-30831.
[20] Stock K, Borrink R, Mikesch JH, Hansmeier A, Rehkämper J, Trautmann M, Wardelmann E, Hartmann W, Sperveslage J and Steinestel K. Overexpression and Tyr421-phosphorylation of cortactin is induced by three-dimensional spheroid culturing and contributes to migration and invasion of pancreatic ductal adenocarcinoma (PDAC) cells. Cancer Cell Int 2019; 19: 77.
[21] Rajadurai CV, Havrylov S, Zaoui K, Vaillancourt R, Stuible M, Naujokas M, Zuo D, Tremblay ML and Park M. Met receptor tyrosine kinase signals through a cortactin-Gab1 scaffold complex, to mediate invadopodia. J Cell Sci 2012; 125: 2940-2953.
[22] Pan YR, Cho KH, Lee HH, Chang ZF and Chen HC. Protein tyrosine phosphatase SHP2 suppresses podosome rosette formation in Src-transformed fibroblasts. J Cell Sci 2013; 126: 657-666.
[23] Olea-Flores M, Zuñiga-Eulogio MD, Mendoza-Catalán MA, Rodríguez-Ruiz HA, Castañeda-Saucedo E, Ortuño-Pineda C, Padilla-Benavides T and Navarro-Tito N. Extracellular-signal regulated kinase: a central molecule driving epithelial-mesenchymal transition in cancer. Int J Mol Sci 2019; 20: 2885.
[24] Mondal S, Adhikari N, Banerjee S, Amin SA and Jha T. Matrix metalloproteinase-9 (MMP-9) and its inhibitors in cancer: a minireview. Eur J Med Chem 2020; 194: 112260.
[25] Sinha S, Hoshino D, Hong NH, Kirkbride KC, Grega-Larson NE, Seiki M, Tyska MJ and Weaver AM. Cortactin promotes exosome secretion by controlling branched actin dynamics. J Cell Biol 2016; 214: 197-213.
[26] Beghein E, Devriese D, Van Hoey E and Gettemans J. Cortactin and fascin-1 regulate extracellular vesicle release by controlling endosomal trafficking or invadopodia formation and function. Sci Rep 2018; 8: 15606.

[27] Kodama T, Newberg JY, Kodama M, Rangel R, Yoshihara K, Tien JC, Parsons PH, Wu H, Finegold MJ, Copeland NG and Jenkins NA. Transposon mutagenesis identifies genes and cellular processes driving epithelial-mesenchymal transition in hepatocellular carcinoma. Proc Natl Acad Sci U S A 2016; 113: E3384-3393.
[28] Lugano R, Ramachandran M and Dimberg A. Tumor angiogenesis: causes, consequences, challenges and opportunities. Cell Mol Life Sci 2020; 77: 1745-1770.
[29] Zhang XP, Li KR, Yu Q, Yao MD, Ge HM, Li XM, Jiang Q, Yao J and Cao C. Ginsenoside Rh2 inhibits vascular endothelial growth factor-induced corneal neovascularization. FASEB J 2018; 32: 3782-3791.
[30] Silva JAF, Qi X, Grant MB and Boulton ME. Spatial and temporal VEGF receptor intracellular trafficking in microvascular and macrovascular endothelial cells. Sci Rep 2021; 11: 17400.
[31] Li J, Qin S, Xu J, Xiong J, Wu C, Bai Y, Liu W, Tong J, Liu Y, Xu R, Wang Z, Wang Q, Ouyang X, Yang Y, Ba Y, Liang J, Lin X, Luo D, Zheng R, Wang X, Sun G, Wang L, Zheng L, Guo H, Wu J, Xu N, Yang J, Zhang H, Cheng Y, Wang N, Chen L, Fan Z, Sun P and Yu H. Randomized, double-blind, placebo-controlled phase III trial of apatinib in patients with chemotherapy-refractory advanced or metastatic adenocarcinoma of the stomach or gastroesophageal junction. J Clin Oncol 2016; 34: 1448-1454.